Journal of Sound and Vibration (1999) **228**(5), 1182–1194
Article No. jsvi.1999.2468, available online at http://www.idealibrary.com on IDEAL®

TRADEOFFS IN DESIGN COMPLEXITY — TEMPORAL VERSUS SPATIAL COMPENSATION

G. C. Smith and R. L. Clark

Department of Mechanical Engineering and Materials Science, Duke University, Durham, NC 27708-0302, *U.S.A.*

(*Received* 11 *June* 1999)

1. INTRODUCTION

In adaptive structure design there are two general approaches to increase the performance of a feedback active control system. One approach is to change the type of temporal compensation or controller implemented. Commonly, a static controller is replaced by a more complex dynamic controller, as they offer the ability to frequency-shape the control signals. However, as detailed by Vipperman and Clark [1], dynamic controllers are more challenging to experimentally implement, due to the required programming and use of digital signal processor (DSP) boards and additional filtering hardware. The other approach to increase adaptive structure performance is to optimize the spatial compensation of the active control system. Many authors have accomplished this by developing techniques to determine the optimum transducer placement on the structure [2–5], and the results have demonstrated significant performance increase.

It is the purpose of this letter to consider the design of controllers and optimum spatial placement of transducers, both individually and concurrently, and to compare the achievable performance increases. This investigation will give practitioners an understanding of the tradeoffs in design complexity between optimizing temporal compensation versus optimizing spatial compensation. As with previous design work by the authors in reference [6], a level basis for comparison of the closed-loop performance results is created by adjusting each design such that the adaptive structures use the same level of control signal energy. The design processes and other theoretical developments are discussed in section 2. The physical test system is detailed in section 3. The results of the design cases are presented and discussed in section 4. Conclusions of this work are given in section 5.

2. THEORY

This letter represents a multi-disciplinary investigation in structural acoustic modelling, performance metrics, optimal temporal compensation design and optimal spatial compensation design. Theoretical developments new to this work

0022-460X/99/501182 + 13 $30.00/0

are detailed below. However, due to space constraints, previous developments are appropriately referenced.

2.1. STRUCTURAL ACOUSTIC MODEL

A structural model of a simply supported plate with attached distributed transducers is built using the assumed modes approach, as outlined by Clark *et al.* [7]. A diagram of the test plate and control system hardware is given in Figure 1. A total of three sensoriactuator [1] transducers are attached to the plate for structural acoustic control, with the localized mass and stiffness effects of each transducers incorporated into the plate model. Using the appropriate sensoriactuator hardware, each transducer acts as a colocated sensor–actuator pair. Implementation issues associated with the sensoriactuator are not considered here, but are detailed by Vipperman and Clark [1]. Finally, further details on the transducer and plate physical properties are given in section 3.

A new development in this work, is the assumption that each plate mode is excited at the same input level, weighted by its modal mass. In standard state-space notation [7], this is defined as

$$\mathbf{Bu} = \begin{bmatrix} 0 \\ [\mathbf{M}_s + \mathbf{M}_p]^{-1} \end{bmatrix} \mathbf{u}, \tag{1}$$

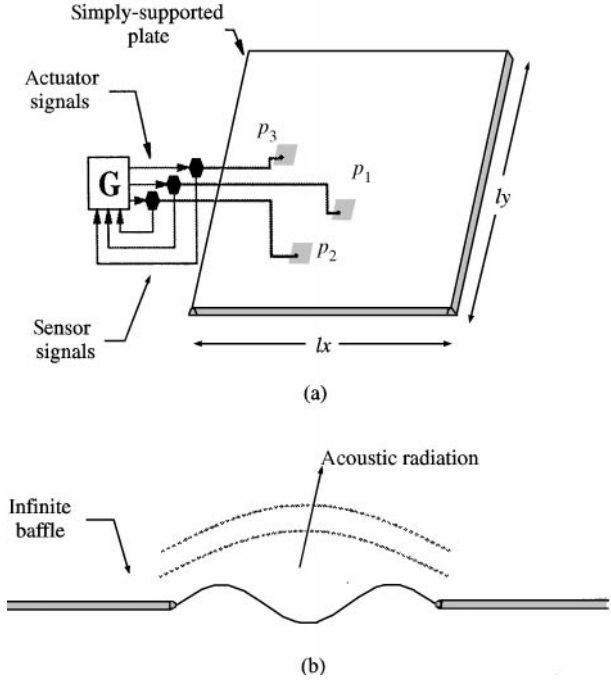

Figure 1. Simply supported plate test structure with three small sensoriactuator transducers (arbitrary or non-optimal position): (a) front view, (b) side view; ▬, 0·0508 × 0·0508 m piezoceramic patch; ⬣, Sensoriactuator hardware; G Controller.

where $\mathbf{u}$ is the $N_m \times 1$ input disturbance vector, N_m is the number of structural modes included in the model, $\mathbf{M}_s$ and $\mathbf{M}_p$ are the $N_m \times N_m$ mass matrices associated with the structure and transducers, respectively, and 0 is a $N_m \times N_m$ matrix of zeros. It is assumed that each input is uncorrelated and has a unity power spectrum, i.e., $S_{uu}(\omega) = 1$. The *generalized disturbance* defined in equation (1) omits the spatial filtering effects of a specific disturbance transducer type or placement. Thus, it is felt that the optimum designs and performance results are more applicable to a wide variety of disturbance scenarios.

In this work, the adaptive structure is designed to reduce the total far-field sound power radiated by the plate due to the input disturbance. Assuming that the plate resides within an infinite baffle and radiates into an infinite half-space (see side-view in Figure 1), Rayleigh's integral can be used to characterize the sound pressure level at a far-field point in terms of the velocity of the vibrating plate surface. Radiation filters are then developed which relate the modal surface velocity of the plate to the total radiated sound power. For this work, the radiation filters detailed by Clark and Cox [8] are utilized. Further details on this portion of the model development are found in reference [8].

2.2. PERFORMANCE METRICS

Design optimization usually involves the minimization of a cost functional which relates to a desired performance goal. A block diagram of the *cost functional system*, $\mathbf{H}(s)$, for this work is shown in Figure 2. The input to the system is generalized disturbance, $\mathbf{u}$. As detailed, $\mathbf{H}(s)$ is comprised of the plate model, controller, radiation filter, and appropriate weighting matrices. Inputs to the plate model are the generalized disturbance and the sensoriactuator control signals, $\mathbf{u}_c$. Outputs of the plate model are the plate modal velocity, $\mathbf{v}$, and the sensoriactuator sensor signals, $\mathbf{y}_s$. The output of the radiation filter, $\mathbf{a}$, is a measure of structural acoustic radiation. The cost functional system has three outputs: one output is the weighted sum, $\mathbf{Z}$, of the structural acoustic radiation signal (performance) and the sensoriactuator control signals (control effort); the other two outputs of $\mathbf{H}(s)$ are the unweighted performance and control effort signals.

Three transfer matrices can be identified through the cost functional system: $\mathbf{H}_{\mathrm{Zu}}(s)$, $\mathbf{H}_{\mathrm{au}}(s)$, and $\mathbf{H}_{\mathrm{u_c u}}(s)$. Each transfer matrix forms an appropriate performance metric for compensation design and analysis. The $\mathscr{H}_2$ norm of $\mathbf{H}_{\mathrm{Zu}}(s)$ forms the performance metric for both spatial and temporal compensation design optimization. The physical interpretation being that the $\mathscr{H}_2$ norm is the r.m.s. value of the weighted output, $\mathbf{Z}$, when the generalized disturbance inputs are driven concurrently by independent, spectrally white noise (see equation (1) above) [9].

For optimum spatial compensation design, the placement of the three colocated transducers is varied on the plate surface until the $\mathscr{H}_2$ norm of $\mathbf{H}_{\mathrm{Zu}}(s)$ is minimized. For optimum temporal compensation design, the $\mathscr{H}_2$ norm of $\mathbf{H}_{\mathrm{Zu}}(s)$ is minimized by the proper selection of $\mathbf{G}$. Two controller forms are being considered: a static $\mathbf{G}$ comprised of a constant 3×3 gain matrix and a dynamic $\mathbf{G}(s)$ which includes a full system model.

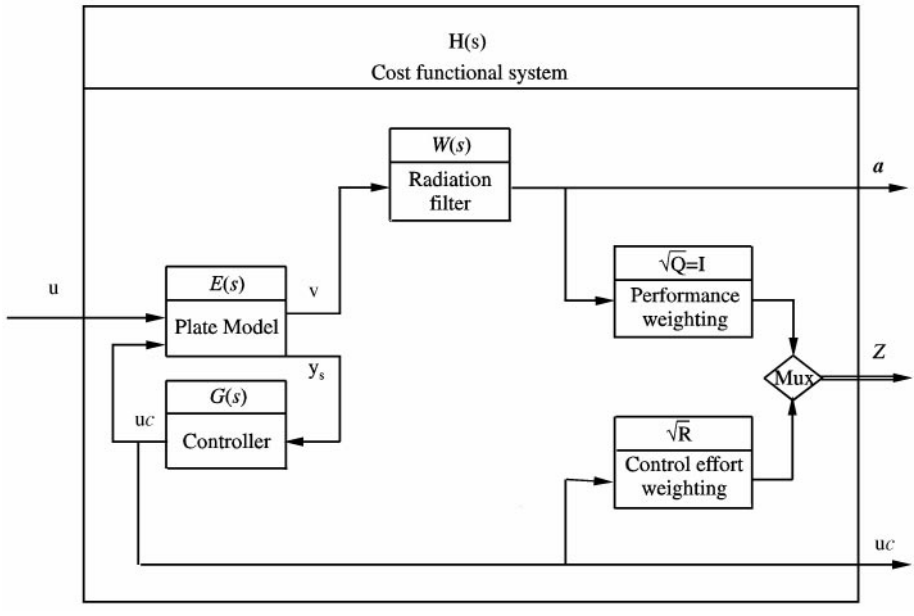

Figure 2. Block diagram of cost functional system for compensator design nd analysis.

The weighted output, **Z**, of the cost functional system provides for a metric which is a balance of both performance and control effort. As detailed in Figure 2, the performance weighting is simply an appropriately sized identity matrix. However, the coefficient **R** is adjusted for each design to ensure that all control systems use the same level of control signal energy [6].

The two other transfer matrices through $\mathbf{H}(s)$ are used to analyze the optimum temporal and spatial compensation designs. The $\mathscr{H}_2$ norm of $\mathbf{H}_{u_c u}$ provides a measure of the control signal energy per unit of disturbance. Whereas, the $\mathscr{H}_2$ norm of $\mathbf{H}_{au}$ forms a metric that compares the structural acoustic control performance of the different design configurations. Called active insertion loss [10], the reduction of noise transmission by the activation of the each control system is characterized as $AIL \equiv 20 \log_{10}(T_{ol}/T_{cl})$. The term T_{ol} is the $\mathscr{H}_2$ norm of the open-loop performance transfer matrix ($\mathbf{H}_{au}$ where $\mathbf{G}(s) = 0$) over the bandwidth of interest and T_{cl} is the $\mathscr{H}_2$ norm of the closed-loop performance transfer matrix over the same bandwidth. Thus, positive values of AIL correspond to a reduction in radiated sound power.

2.3. OPTIMUM TEMPORAL COMPENSATION DESIGN

Two controller types are being considered in this work: static, output feedback and dynamic, $\mathscr{H}_2$ control. Using iterative optimization schemes, each controller type is designed to provide maximum reduction of the $\mathscr{H}_2$ norm of $\mathbf{H}_{Zu}$. The static, output feedback controller is designed using the dual Levine–Athans (DLA)

algorithm [11] and the dynamic $\mathscr{H}_2$ controller is designed using the state-space solutions prescribed by Doyle *et al.* [12].

2.3.1. *Static, Output Feedback Control*

Frequency-independent, static, output-feedback controllers are often desirable for adaptive structures due to their robustness with respect to parametric model uncertainty and minimal hardware requirements (i.e., analog resistors and amplifiers). Many techniques have been proposed to determine the optimum constant gain matrix and the dual Levine–Athans (DLA) algorithm is used here. The DLA algorithm was first described by Levine and Athans [11] and later applied to structural acoustic control by Clark and Cox [8]. The algorithm is globally convergent (i.e., converges from any initial stabilizing feedback gain to stationary point of the cost functional) and the solution satisfies the necessary conditions for optimality.

2.3.2. *$\mathscr{H}_2$ Control*

Similar to the static, output feedback control design process, $\mathscr{H}_2$ control involves the minimization of the $\mathscr{H}_2$ norm of $\mathbf{H}_{Zu}$. The primary advantage of $\mathscr{H}_2$ control is that the controller's action can vary as a function of frequency. This offers increased closed-loop performance and increased design flexibility. Further, $\mathscr{H}_2$ control designs also have a reduced sensitivity to signal uncertainty when compared to other dynamic control techniques, e.g., LQG control. The $\mathscr{H}_2$ control design problem is solved using the state-space solutions presented in reference [12]. This process involves solving two Riccatti equations by Schur decomposition and realizes a full dynamic controller, $\mathbf{G}(s)$, with its own set of poles and zeros. The optimal solution is unique and has a dimension equal to that of $\mathbf{H}_{Zu}$. The solution is also stable, proper, and hence realizable.

2.4. OPTIMUM SPATIAL COMPENSATION DESIGN

The design of the spatial compensation of the control system is optimized using the techniques developed in reference [4]. This approach uses sequential quadratic programming (SQP) to determine a set of transducer locations that minimize the $\mathscr{H}_2$ norm of $\mathbf{H}_{Zu}$. SQP is a non-linear programming method based upon the iterative formulation and solution of quadratic subproblems and, as shown in reference [4], is rapidly convergent. Its application to optimizing spatial compensation of active control applications has been recently verified by De Fonseca *et al.* [5].

A difference between this work and that in reference [4] is that here distributed piezo-electric transducers are utilized; reference [4] utilized point transducers. As such, a design constraint relating to transducer overlap must be added to the optimization process. Wang *et al.*, [13] presented a transducer overlap constraint based upon approximating the square/rectangular patches as circular areas. For this work, a constraint based upon the infinity-norm is developed. The advantage

of this approach is that edge-to-edge patch placement is allowed and the number of overlap constraint equations has been reduced from three to one.

Assuming that the origin is at the lower-left corner of the plate and normalized dimensions, the infinity-norm overlap constraint is written as

$$G_{i,j} = -\left(\left\| \frac{x_i - x_j}{l_x^p}, \frac{y_i - y_j}{l_x^p} \right\|_\infty - 1\right), \tag{2}$$

where $G_{i,j}$ is the constraint between transducers i and j, i $\neq$ j, (x_i, y_i) and (x_j, y_j) are the non-dimensional center locations of each transducer and (l_x^p, l_y^p) are characteristic dimensions of the square/rectangular transducers. In this development, it is also assumed that the transducer patches are always oriented square to the plate edges.

Another constraint is necessary to ensure that the patches are placed within the plate boundaries. Again using the infinity norm, the edge constraints are written as

$$G_i = \|x_i - 1/2\|_\infty + l_x^p/2 - 1/2, \tag{3a}$$

$$G_i = \|y_i - 1/2\|_\infty + l_y^p/2 - 1/2, \tag{3b}$$

where G_i is the edge constraint for the ith transducer. The use of the infinity-norm approach reduces the number of edge-constraint evaluations by a factor of two from traditional methods that evaluate each edge individually [13,4], e.g., equation (3b) replaces $x_j - l_x^p/2 < 0$ and $x_j + l_x^p/2 - 1 < 0$.

3. PHYSICAL SYSTEM

The plate shown in Figure 1 is assumed to have simply supported boundary conditions and be made of steel. The plate material properties are given in Table 1. Each control transducer is assumed to be a square patch of distributed PZT material; the transducer material properties are given in Table 2. The transducer placement shown in Figure 1 has been arbitrarily selected. Throughout the rest of this work, this is referred to as the *non-optimal* placement. The non-optimal placement is also the initial placement for the optimum spatial compensator design process. The non-optimal center locations of each transducer are given in the first column of Table 3, and noted as X_0. The center points are being reported in non-dimensional terms, $(x/l_x^s, y/l_y^s)$. The last two columns of Table 3 give the optimal placement, X_{opt}, for the two controller cases. These results are discussed in section 4.

The following parameters are held constant for each of the design cases: the number of structural modes in the plate model, $N_m = 30$; the number of structural modes incorporated into the radiation filters, $N_f = 10$; and the DLA algorithm convergence parameter [8], $\varepsilon = 1 \times 10^{-2}$. A larger number of plate modes is utilized to sufficiently converge the plate zeros over the selected bandwidth of interest: 0–500 Hz. However, the number of modes used in forming the radiation filters need only be extended over the desired bandwidth. The 0–500 Hz frequency band represents the design region in which plate acoustic energy is a maximum and passive noise control techniques are least effective.

TABLE 1

Properties of plate test structure

Property	Value
Material	Cold-rolled steel
Width, l_x^s	0·600 m
Height, l_y^s	0·525 m
Thickness, l_z^s	0·002 m
Density, ρ_s	7700 kg/m^3
Young's modulus, E_s	$19{\cdot}5 \times 10^{10}$ Pa
Poisson's ratio, v_s	0·2
Damping ratio, ζ	0·05

TABLE 2

Properties of distributed transducers

Property	Value
Material	G-1195 PZT
Width, l_x^p	0·0508 m
Height, l_y^p	0·0508 m
Thickness, l_z^p	0·0002 m
Density, ρ_p	7650 kg/m^3
Young's modulus, E_p	$4{\cdot}9 \times 10^{10}$ Pa
Poisson's ratio, v_p	0·3
Strain coefficients, d_{31}	-66×10^{-12} m/V

TABLE 3

Placement of distributed transducer centers

Patch	Non-optimal X_O	Location (m/m) Static, Optimal X_{opt}	$\mathscr{H}_2$ Optimal X_{opt}
p_1	(0·50, 0·32)	(0·63, 0·57)	(0·64, 0·23)
p_2	(0·45, 0·15)	(0·51, 0·35)	(0·44, 0·25)
p_3	(0·28, 0·57)	(0·37, 0·60)	(0·43, 0·73)

4. RESULTS AND DISCUSSION

The performance results of four temporal and spatial compensation design cases are compared in this work: two cases with a static controller and two cases with a dynamic controller. For each controller, one case is with the non-optimal transducer placement and one case is with optimal transducer placement. The non-optimal transducer placement is chosen as the same for both controllers.

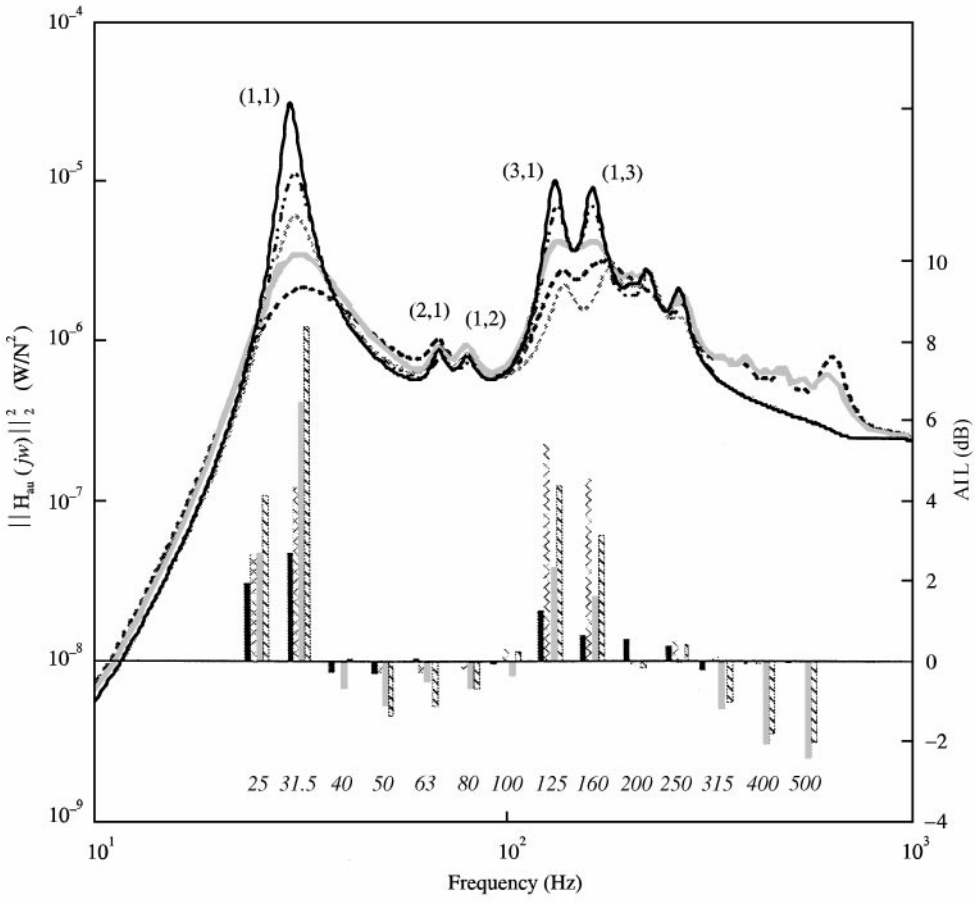

Figure 3. Acoustic power spectrum and AIL for all control system design cases (modal indices, (i_x, j_y), are shown in parenthesis and 1/3-Octave band center frequencies are shown in italics): —, open-loop; – · · – ■, closed-loop, static, non-optimal location; · · · · ▨, closed-loop, static optimal location, equal control energy; —— ■, closed-loop, H2, non-optimal location, equal control energy; – – – – ▨, closed-loop, H2, optimal location,equal control energy.

However, results show that the optimal transducer placement varies for static and dynamic controllers.

The acoustic performance results for all design cases are plotted in Figure 3. Each curve represents the acoustic power radiated per unit of input disturbance, over the frequency band of interest. The top, solid line is the open-loop response of the system, where the control transducers are attached (non-optimal placement), but not activated. The sharp peaks in the plate acoustic response correspond to the structural modal resonances; the modal indices, (i_x, j_y), of each peak are shown in parenthesis in Figure 3. The four lower curves show the acoustic performance when each control system has been activated. The active insertion loss (AIL) in 1/3-octave bands of each design case is also given in Figure 3. The AIL ordinate is shown on the right of the figure and the 1/3-octave band center frequencies are shown in italics. A detailed discussion of the performance results for each design case is given below.

4.1 STATIC, OUTPUT FEEDBACK CONTROL

The first two design cases considered are when **G** is a 3×3 static matrix. Static controllers are desirable for adaptive structures due to their simplicity and ease of implementation. However, as shown below, static controllers have performance limitations.

The closed-loop response of the static controller with non-optimal transducer placement case is shown as the dashed-dot-dot line in Figure 3. Small reductions in the response of the strong acoustic radiator modes are shown with this control system. The AIL results detail a 2·7 dB reduction in the 1/3-octave band centered at 31·5 Hz. The 31·5 Hz 1/3-octave band includes the fundamental (1,1) plate mode, which is at 29·8 Hz. The static, non-optimal placement case also provides control of the next two strong acoustic radiators: the (3,1) mode at 133·4 Hz and the (1,3) mode at 165·0 Hz. The AIL results show 1·2 dB of reduction in the 1/3-octave band at 125 Hz and 0·6 dB in the 1/3-octave band at 160 Hz. These performance results, along with those for the other three design cases, are summarized in Table 4, where it is also shown that the static, non-optimal placement design case provides 1·6 dB of reduction over the entire frequency band of interest.

The eigenvalues of the static controller with non-optimal transducer placement are all positive and real. Thus, this design of a colocated, strain-rate feedback system is dissipative, with the associated guarantee of stability and excellent robustness to model uncertainty [7,8].

The static, non-optimal placement case also sets the baseline of control energy for this work; the parameter **R** for the other three cases is adjusted such that they utilize the same amount of control energy as this case. Table 5 gives the control energy results for the four design cases. The first column shows that with $\mathbf{R} = 6{\cdot}929 \times 10^{-15}$ the static controller with non-optimal transducer placement has a control signal energy level of $459{\cdot}832 V/N$. As discussed in reference [6], this signal level is reasonable for practical control system implementation. The weightings and resulting signal levels for the other design cases are also given in Table 5. For each case, the value of **R** was adjusted to normalize the control signal energy to within $\pm 0{\cdot}001 V/N$ of $59{\cdot}832 V/N$. The proper values of **R** were realized by employing a linear, numerical line search routine.

TABLE 4

AIL of control system designs in selected 1/3*-octave bands and over the entire* 0–500 *Hz bandwidth*

	AIL (dB)			
1/3-octave (Hz)	Static, X_O	Static, X_{opt}	$\mathscr{H}_2$, X_O	$\mathscr{H}_2$, X_{opt}
31·5	2·7	4·3	6·4	8·4
125	1·2	5·4	2·3	4·4
160	0·6	4·5	1·6	3·1
Overall	1·6	2·4	2·8	3·4

TABLE 5

Control effort weighting and resulting control power for each control system design

	Static, X_O	Static, X_{opt}	$\mathscr{H}_2$, X_O	$\mathscr{H}_2$, X_{opt}
R	$6{\cdot}929 \times 10^{-15}$	$8{\cdot}3473 \times 10^{-15}$	$4{\cdot}5400 \times 10^{-18}$	$4{\cdot}7707 \times 10^{-8}$
$\|\mathbf{H}_c\|_2$ (V/N)	459·832	459·833	459·833	459·833

As discussed in reference [6], static controllers do not offer the ability to frequency-shape the sensor response. Therefore, it is expected that optimizing the spatial compensation design of an adaptive structure with a static controller will offer a significant performance increase. Starting with the non-optimal transducer placement, the techniques presented in section 2.3. are applied to the static controller case. The optimal transducer placement was determined in 87 design iterations and is given in the second column of Table 3.

The acoustic performance results of the static controller with optimal transducer placement and normalized control energy, are given in Figure 3 and Table 4. As expected, optimizing transducer placement has significantly increased the performance of the static control system. The 1/3-octave band response at 31·5 Hz, has reduced 4·3 dB from the open-loop response and 1·6 dB from the non-optimal case. Even greater increases are shown in controlling the responses of the higher radiating modes. For the 1/3-octave band at 125 Hz, the acoustic response has reduced 5·4 dB from the open-loop case and 4·2 dB from the non-optimal placement case. Overall, the static controller with optimal transducer placement provides 2·4 dB of reduction integrated over the bandwidth – a 0·8 dB improvement from the non-optimal case. The eigenvalues of the static controller for the optimal transducer locations are also all positive and real; this design yields a positive-real, dissipative controller.

4.2. $\mathscr{H}_2$ CONTROL

The $\mathscr{H}_2$ control design is implemented to investigate the performance increase gained from a dynamic controller. In this formulation, the controller involves a full system model with 248 states.

To ensure robustness of the $\mathscr{H}_2$ controller, random measurement noise is assumed on all three sensors during controller design. Each noise signal is an uncorrelated zero-mean Gaussian stochastic process with a constant power spectral density of $S_{vv}(\omega) = 7{\cdot}0 \times 10^{-5}$. This value corresponds to a noise level that is approximately 10% of the sensor signal levels, during operation in their non-optimal positions.

The $\mathscr{H}_2$ control is first evaluated with non-optimal transducer placement. The results for this case are shown as the solid gray line in Figure 3 and summarized in Table 4. The $\mathscr{H}_2$ controller with non-optimal transducer placement shows significantly greater control of the plate response than the static controller with non-optimal placement, even with normalized control energy. In each of

the 1/3-octave bands of interest, the performance of the $\mathscr{H}_2$ controller with non-optimal placement is greater than twice that of the static controller with the same transducer placement.

Comparison of the results for the $\mathscr{H}_2$ controller with non-optimal transducer placement and the results for the static controller with optimal transducer placement show similar performance improvements, owing to the operation of the induced strain transducers. Over the frequency band of interest, the static controller with optimal transducer placement provides 2·4 dB of reduction; whereas, the $\mathscr{H}_2$ controller with non-optimal transducer placement provides 2·8 dB of reduction. Control of the fundamental mode is significantly greater using the $\mathscr{H}_2$ controller with non-optimal transducer positions. However, the static controller with optimal transducer positions provides greater control of the higher acoustic radiators.

Using the spatial optimization routine, the transducer placement of the $\mathscr{H}_2$ controller is optimized. The optimal placement for the $\mathscr{H}_2$ controller was determined in 124 design iterations and is given in the last column of Table 3. The optimal placement for the $\mathscr{H}_2$ controller is different from the optimal placement for the static controller case. Results in Figure 3 show that control of the fundamental plate mode is greatest with the $\mathscr{H}_2$ controller with optimal transducer placement. However, the higher frequency performance of both the non-optimal and optimal dynamic controller is not as great as the static controller case with optimal placement. This is most likely a result of the dynamic controller giving greater emphasis to the lower frequency range and the fact that the static controller uses induced strain transducers which couple more efficiently to high frequency modes. Whereas, for the dynamic controller the sensor noise limits the high frequency response. Overall reduction of structural acoustic response is significantly greater for the $\mathscr{H}_2$ controller with optimal placement case than all the other cases.

An important comparison is to consider the performance increase from spatial compensation optimization for both the static and dynamic controller cases. Comparison of the 1/3-octave bands of interest in Table 4 shows that a much greater relative increase in performance is obtained for static controllers. Since static controllers have a fixed frequency response, frequency-shaping of the control system is achieved exclusively by varying the spatial compensation. Dynamic controllers offer the ability to frequency shape the control system response, without the need to significantly vary the spatial compensator. Thus, performance increases from spatial placement optimization with a static controller are much more significant.

Finally, Figure 3 shows that the $\mathscr{H}_2$ controller in both transducer placement cases increases the acoustic response of the plate above the frequency range of interest. This behavior is commonly referred to as *controller spillover*. Controller spillover is a significant issue when evaluating a control system as it can lead to system instabilities associated with unmodelled system dynamics. Such issues are not investigated in this work, but must be considered for practical application.

5. CONCLUSIONS

A comparison of the performance of static and dynamic ($\mathscr{H}_2$) controllers with both non-optimal (arbitrary) and optimal transducer placement was conducted. All

design cases were normalized such that each controller utilized the same amount of control signal energy. The results demonstrate that:

(1) optimizing transducer placement for a static controller provides a performance increase comparable to replacing the static controller with a dynamic controller under the constraint of equal control effort;
(2) determining the optimal transducer placement increases the performance of both static and dynamic controllers, where the greatest relative increase is seen with static controllers;
(3) a dynamic controller with optimal transducer placement provides the greatest performance of all the design cases.

Optimizing transducer placement (spatial compensation) should be considered an important aspect of designing an adaptive structure with a static controller, as this process overcomes some of the performance limitations of static controllers. However, if optimal performance is desired it is best to assume the design complexity of both optimizing transducer placement and implementing a dynamic controller.

ACKNOWLEDGMENTS

This work was supported by NSF Career Program CMS-9501470.

REFERENCES

1. J. S. Vipperman and R. L. Clark 1999 *Journal of the Acoustical Society of America* **105**, 219–225. Multivariable feedback active structural acoustic control using adaptive piezoelectric sensoriactuators.
2. J. L. Junkins and Y. Kim 1993 *Introduction to Dynamics and Control of Flexible Structures*. AIAA Education Series. Washington, DC: AIAA.
3. K. B. Lim and W. Gawronski 1993 *Control and Dynamic Systems* **57**, 109–152. Actuator and sensor placement for control of flexible structures.
4. G. C. Smith and R. L. Clark 1997 *AIAA Paper* 97-1316. Optimal transducer placement for output feedback control of broadband structural acoustic radiation.
5. P. De Fonseca, P. Sas and H. Van Brussel 1999 *Journal of Sound and Vibration* **221**, 651–679. A comparative study of methods for optimising sensor and actuator locations in active control applications.
6. G. C. Smith and R. L. Clark 1998 *Journal of the Acoustical Society of America* **104**, 2236–2244. The influence of frequency-shaped cost functionals on the structural acoustic control performance of static, output feedback controllers.
7. R. L. Clark, W. R. Saunders and G. P. Gibbs 1998 *Adaptive Structures, Dynamics and Control*. New York: Wiley.
8. R. L. Clark and D. E. Cox 1997 *Journal of the Acoustical Society of America* **102**, 2747–2756. Multi-variable structural acoustic control with static compensation.
9. S. Boyd and C. Baratt 1991 *Linear Controller Design: Limits of Performance*. Englewood Cliffs, NJ: Prentice-Hall, Inc.
10. G. C. Smith and R. L. Clark 1998 *Noise Control Engineering Journal*, Active insertion loss (AIL) (submitted).

11. W. S. Levine and M. Athans 1970 *IEEE Transactions on Automatic Control* AC-**15**, 44–48. On the determination of the optimal constant output feedback gains for linear multivariable systems.
12. W. C. Doyle, K. Glover, P. P. Khargonekar and B. A. Francis 1989 *IEEE Transactions on Automatic Control* ac-**34**, 831–847. State-space solutions to standard $\mathscr{H}_2$ and $\mathscr{H}_\infty$ control problems.
13. B. T. Wang, R. A. Burdisso and C. R. Fuller 1994 *Journal of Intelligent Material Systems and Structures* **5,** 67–77. Optimal placement of piezoelectric actuators for active structural acoustic control.